Available online at www.sciencedirect.com
ScienceDirect
Journal of Applied Geophysics 62 (2007) 178–191
JOURNAL OF APPLIED GEOPHYSICS
www.elsevier.com/locate/jappgeo

The characterization of trough and planar cross-bedding from borehole image logs

Paul W.J. Glover [a,*], P. Bormann [b]

[a] *Département de Géologie et de Génie Géologique, Université Laval, Québec (QC), Canada G1R 3A9*
[b] *Norske Shell, Postboks 40, 4098 Tananger, Norway*

Received 21 February 2006; accepted 5 November 2006

Abstract

Conventional analysis of borehole images involves fitting sinusoidal curves to borehole/structure intersection curves, and assumes that the sedimentary features are planar. If trough cross-bedding occurs the conventional technique can result in large errors in the direction of the trough axis (up to +35° in dip and ±90° in azimuth) due to the unknown offset between the borehole axis and the trough axis. We present an analytical model describing the curves from the intersection of a vertical borehole with a mathematically generalized trough cross-bedded structure. The new model shows deviations of the trough axis from sinusoidal behavior that increase as the dip and the width of the trough decreases, and as the offset increases. The conventional and new techniques have been compared by using both of them to analyze blindly a set of mixed plane and trough cross-bedded electrical or acoustic image data. This analysis shows that the new technique provides (i) improved accuracy in dip and azimuth determinations, (ii) additional information concerning the width of the trough and the offset, and (iii) enhanced vertical resolution arising because accurate directional data can be obtained for individual structures, enabling each structure to be accurately and uniquely mapped in three dimensions in the sub-surface. The new model may be modified to provide intersection curves between elliptical boreholes with hemi-cylindrical or elliptical sub-surface structures. The limitations of the new model are that its useful applicability is controlled by the resolution of image log data, the size and quality of the borehole, and the use of a centralized tool.

Keywords: Image logs; Paleoflow direction; Trough cross-bedding; Azimuth; Dip; FMI; BHTV

1. Introduction

This paper sets out to analyze intersection curves from image logs that are likely to contain trough-bedded structures with two methods. The first method is that which is followed conventionally by the logging industry and major exploration companies. It involves fitting sinusoidal curves to the image log data and assumes that all structures that intersect the borehole are planar, and provides the apparent dip and azimuth of the plane (Rider, 1996). The second method is developed within this paper. It involves fitting the intersection curves with an equation that has been generated from the analysis of the intersection of a cylindrical borehole with a generalized hemi-cylindrical structure. It assumes that the tool is centralized in the borehole. In principal the mathematical model developed in this paper can be extended to take account of an elliptical borehole, any hemi-elliptical subsurface structure, and non-verticality of the borehole. These extensions will be the subject of further publication.

* Corresponding author.
E-mail address: paglover@ggl.ulaval.ca (P.W.J. Glover).

0926-9851/$ - see front matter © 2006 Published by Elsevier B.V.
doi:10.1016/j.jappgeo.2006.11.001

This method is equally applicable to planar or trough-like structures and provides the dip, azimuth, size and offset position of the structure with respect to the borehole. These data are fundamental to the analysis of paleocurrents, which can provide detailed information concerning the lateral distribution of oil and gas reservoirs by allowing the reconstruction of paleogeographic maps (e.g., Glennie, 1972; Hurley et al., 1994).

The basic assumption in paleocurrent analysis is that bedforms migrate down-current, and hence produce a sequence of inclined foreset laminae that plunge in the direction of flow. The mean direction of transport can be found by measuring the direction of the plunge (azimuth), plotting the azimuth values as rose diagrams, and then calculating their eigenvalues (Curray, 1956) and vector means (Scheidegger, 1965).

As bedforms migrate, they fill local hollows in the morphology of the depositional system, such as a river channel, or they aggregate laterally on a point bar surface (Pettijohn et al., 1987). During this process of net deposition the cross-beds form. Several types of cross-bedding occur, which can be broadly classified as (i) planar/tabular, (ii) trough, (iii) hummocky, and (iv) mixed, and can develop a significant complexity (Lofts et al., 1997).

For planar and tabular cross-bedding the foresets are near parallel and dip in the direction of the paleoflow between 10° to 35°, while the bounding surfaces have a much lower dip (0°–10°).

Trough cross-beds form where higher flow intensities are present (Rubin, 1987) which cause erosional scours at the base of the slip slope of transverse bedforms (Pettijohn et al., 1987). The trough cross-bedding comprises a scoop-shaped or cylindrical scour filled by curved foreset laminae, with the axis of the scoured trough and the crescentic fill laminae oriented parallel to the local principal flow direction (Trexler and Cashman, 1990). The trough-shaped basal scour surfaces form the bounding surfaces of the sedimentary packages, and have a low dip (0° to 15°) that increases in the direction of sediment transport (Cameron et al., 1993; Rider, 1996). The foreset laminae are also trough-shaped, and have dips ranging between 10° and 35° in the direction of paleoflow (Trexler and Cashman, 1990). The foreset surfaces can, in most cases, be described as cylindrical (Singerland and Williams, 1979; DeCelles et al., 1983), but channel trough-beds are also known to occur with elliptical cross-section with half-width to thickness ratios of 4.25 and 5.2, and also with non-axisymmetric cross-sections (Robinson and McCabe, 1997). It should also be noted that it is rare that a full hemi-cylindrical cross-section is found as subsequent erosion normally removes much of the original trough deposit, leaving just the lowermost parts of the hemi-cylinder.

A range of cross-bedding styles can be observed using electrical or acoustic image techniques (e.g., Borehole Televiewer (BHTV)). Conventionally, such imaging data are analyzed by fitting blindly sinusoidal curves to layers of the same resistivity on the unwrapped borehole image. This procedure works well for plane cross-bedded structures such as foresets and set bounding surfaces in planar/tabular cross-bedding. It also works approximately for set bounding surfaces and foreset surfaces in trough cross-bedding if the borehole intersects the axis of the trough by chance.

However, the common case is that the borehole axis intersects the trough at some unknown offset from the trough axis. In this case it is clear that the planar assumption will lead to overestimations in dip and inaccuracies in azimuth of the axis of both the basal trough-bounding surface and its foreset layers that are caused by the steeper trough flanks. The errors in azimuth are a recognized problem that result in broader, more variable azimuth rose diagrams, and azimuth histograms where the trough foresets cannot be distinguished from the set-bounding surfaces. This variability is corrected for approximately by obtaining the vector mean azimuth from a depth interval, and assuming that the errors in azimuth caused by the trough sides cancel out evenly (Rider, 1996). Such a procedure requires a set of azimuthal data for a depth interval commonly greater than 30 m, in which the lithology and structural style of the sediment does not vary. The vector means therefore have a low depth resolution.

2. Intersection curves

Only perfectly planar bedding surfaces produce a true sinusoidal signature in image logs. All other non-planar surfaces produce curves which represent smooth oscillations, and may even appear similar to sinusoidal curves, but they are not sinusoidal. The deviation of these curves from the true sinusoid is a direct function of the deviation of the bedding surface from a perfect plane (Fig. 1).

If a vertical borehole intersects a plane structure of dip $\theta = 10°$ and azimuth $\alpha = 0°$ (Fig. 1a), the intersection curve on the electric or acoustic image data appears as a sinusoidal curve with its minimum in the direction of the maximum dip (i.e., the azimuth of the plane), and its amplitude being related to the size of the dip (Fig. 1b). The z values span $z = 0$, which is the depth at which the borehole axis intersects the plane.

If the same vertical borehole intersects a trough with a trough axis dip $\theta = 10°$, azimuth $\alpha = 0°$, and at some

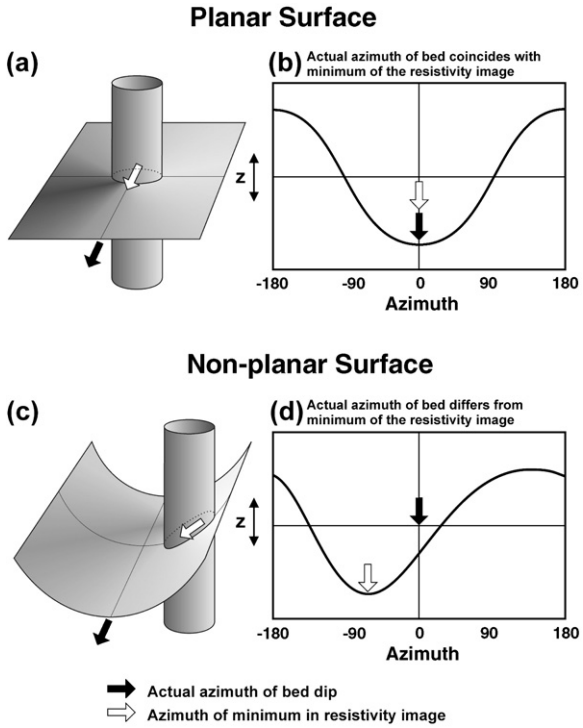

Fig. 1. Representation of planar and non-planar (trough-bedded) borehole images on a flat surface. (a) Borehole intersects a planar structure (dip=10°, azimuth=0°), and (b) the resulting sinusoidal intersection curve. (c) Borehole intersects a non-planar (trough) structure (dip=10°, azimuth=0°, arbitrary trough width and offset), and (d) the resulting non-sinusoidal intersection curve. Solid arrows represent the actual azimuth, open arrows represent apparent azimuth (angle of greatest dip around the borehole).

offset from the trough axis (Fig. 1c), the intersection curve is no longer sinusoidal (Fig. 1d). The minimum of this curve shows the azimuth of the local maximum dip at the borehole, which is not the same as the paleoflow direction along the azimuth of the trough axis. The amplitude of the curve is still related to the dip of the trough axis, but it is also a function of the trough width and the offset between the borehole axis and trough axis. In both cases, it is assumed that the tool is centralized in the borehole.

If the mathematical form of the intersection curve between the borehole and a generalized trough cross-bedded structure can be obtained and fitted to an observed intersection curve, we have a technique for obtaining accurately (i) the trough axis dip, (ii) the trough axis azimuth, (iii) the position of the trough axis with respect to the borehole, and (iv) the width of the trough, for the individual structure. This approach is only practical for small trough cross-bedded structures. For larger ones, the trough becomes increasingly indistinguishable from a planar structure, and this will be apparent from the fitted parameters.

In this paper we recognize that fitting a simple sinusoid is often an oversimplification. Instead we model the trough-bedded structure as an inclined hemicylinder, which is cut by a vertical cylinder representing the borehole. The following sections examine the model intersection curves derived from the conventional and the new approaches. Subsequently, we apply the new technique to electric image log data by using both the new equation and the sinusoidal model in order to distinguish between trough cross-bedded and plane cross-bedded structures and to characterize the geometries of the intersected troughs. In each case we have applied statistical measures of goodness of fit.

It should be noted that the new approach is not a stand-alone technique, but the use of a more general equation within the conventional method for image log analysis, and hence should be simple to incorporate into professional procedures.

3. A new non-planar approach

Unlike the conventional approach, we do not assume that every structure penetrated by the borehole is planar. Instead, we fit a generalized equation, which is equally applicable to both planar and axisymmetric hemicylindrical trough-like structures, to each intersection

curve. We obtain this generalized equation by analyzing the three dimensional geometry of the intersection between a generalized axisymmetric hemi-cylindrical trough cross-bedded structure and a vertical borehole with a circular cross-section. The generalized equation is given by (Appendix A)

$$z = -\frac{1}{\cos\theta}\left[\sin\theta\cos(\alpha-\varphi) + \sqrt{d^2-(\sin(\alpha-\varphi)-b)^2}\right]. \quad (1)$$

The parameters of Eq. (1) are shown diagrammatically in Fig. 2. In this equation z is the distance of the locus of the bed (axial to the borehole) as a function of the angular distance around the borehole α. The ordinate z is also a function of the true dip of the structure θ, the diameter ratio d, the offset ratio b and a phase lag φ. The true dip θ is the dip of the plane or the trough that intersects the borehole in the azimuth direction. The diameter ratio d describes the width of the trough normalized to the diameter of the borehole and has no units. Consequently, a value of $d=1$ represents a trough which has a diameter equal to that of the borehole intersecting it, while the trough becomes planar as $d\rightarrow\infty$. In practice values of d larger than about 25 can be considered as approaching planar behavior. Most trough-bedded systems that can be recognized on image logs have values of d between 1 and 15. Values of d greater than 25 occur for trough-bedded systems that are approaching planar behavior. The offset ratio b is the perpendicular distance between the trough axis and the borehole axis divided by the borehole radius and also has no units. It describes the effect of the borehole intersecting the trough structure at some position which is not on the axis of the trough. It is interesting to note that for the case the true dip $\theta=0$, if the diameter ratio is much greater than the offset ratio (i.e., $d \gg b$), Eq. (1) gives a value of $z=-d$. The phase lag φ is a variable that arises due to lack of a priori knowledge of the absolute direction of $\alpha=0°$. It has been included to ensure that Eq. (1) is completely generalized.

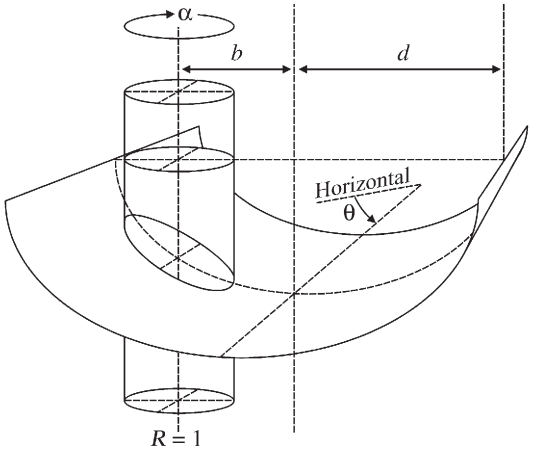

Fig. 2. The geometry and the parameters used in the derivation of the mathematical model for the intersection curve of a single vertical cylindrical borehole of unit diameter, and a hemi-cylindrical trough with a given diameter ratio d, dip θ and trough axis azimuth ψ, at an offset described by an offset ratio b as a function of azimuth α.

This simple analytical equation for the general case of a plane or trough cross-bedded structure of any location, size, dip and azimuth intersecting a borehole with a defined location, size, dip and azimuth can be fitted easily to individual intersection curves from image logs, with a range of statistical measures of accuracy. The fitting procedure allows the dip and azimuth of the sub-surface structure to be obtained, together with information describing the width of the trough and the relative position of the trough axis and the borehole axis. Because it is purely analytical, the new method requires no assumptions other than the trough surfaces and the borehole are approximately cylindrical. As the technique can be applied uniquely to each intersection curve, it has a spatial resolution equal to the resolvable bed scale in the original images.

4. Characteristics of the new model

We compare the new model with the case of a plane cross-bedded horizon while varying each of the three independent parameters in the new model (dip θ, diameter ratio d, and offset ratio b). Figs. 3–5 show examples of intersection curves for trough cross-bedded structures of varying dip θ (Fig. 3), trough diameter ratio d (Fig. 4), and offset ratio b (Fig. 5). In each case the corresponding plane cross-bedded data is shown for comparison. It should be noted that the apparent paleocurrent azimuth by conventional sinusoidal fitting is indicated by the angle at which the intersection curve is at a minimum, but the actual paleocurrent direction in all cases is 0°.

Eq. (1) describes the intersection between the borehole and the trough structure. Consequently, if one would like to compare curves for different dips, diameter ratios or offset ratios, the curves will be translated vertically one from another, and that translation could be significantly larger than the amplitude of the intersection curve. In order to ease the comparison of the shapes of the curves for each case, we have chosen to remove the contribution to the vertical position of the intersection curve that is independent of azimuth so that the azimuth-dependent contribution can be compared.

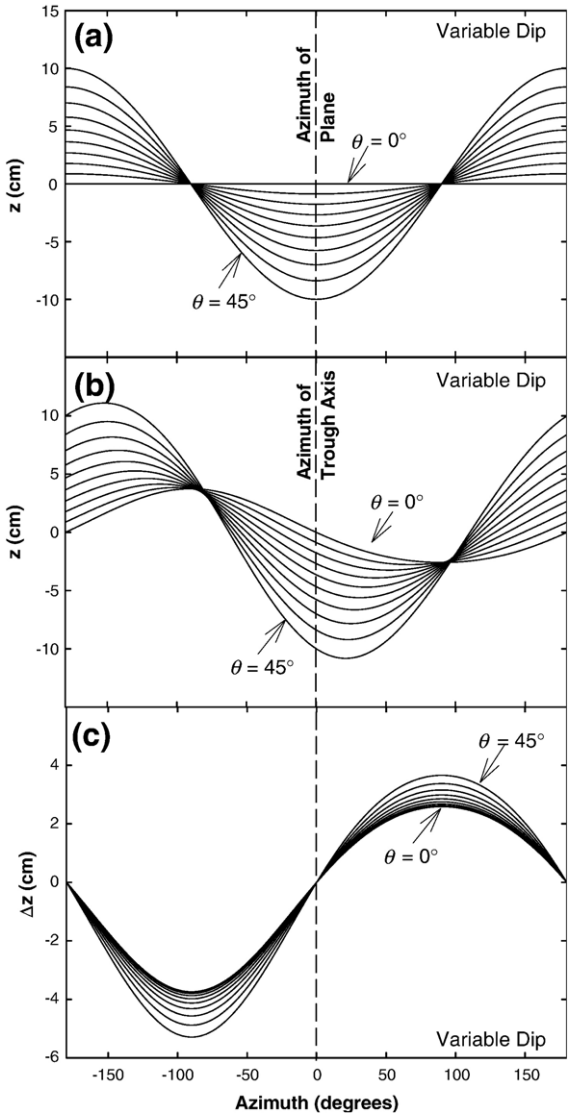

Fig. 3. Forward modeled intersection curves from (a) the sinusoidal model (planar beds), and (b) the trough cross-bedded model (non-planar beds), as a function of dip (θ=0° to 45° in increments of 5°) and as a function of azimuth α. In both cases the azimuth of the plane or trough (i.e., paleocurrent direction) ψ_{axis}=0°. For the trough model, the diameter ratio d=10, and the offset ratio b=3 are held constant. (c) The difference between the sinusoidal model and the trough cross-bedded model as a function of dip and azimuth α.

This has been effected by adding a term that is constant for any given set of dip, and d and b ratios. The addition of this term gathers all the curves so that they all pass through the same value at α=0° and have approximately the same mean value. The correction is given by

$$z' = \sqrt{\frac{d^2 - b^2}{\cos^2\theta}}, \tag{2}$$

where,

$$z = z' + z''(f(\alpha)). \tag{3}$$

The appendix explains that Eq. (1) is written in terms of the ratio of trough diameter and the horizontal offset to the borehole diameter. Consequently, it gives the locus of the intersection curve as the ratio of the vertical position to the borehole diameter, and one must mutiply its result by the borehole diameter to obtain the intersection curves in physical units. The curves shown in Figs. 3–5 represent the result of Eq. (1) multiplied by an arbitrarily chosen borehole diameter of R=10 cm, to provide the final curves in units of centimeters.

Fig. 3 shows intersection curves for both the plane cross-bedded and the trough cross-bedded cases as a function of dip (θ=0° to 45° in 5° increments) with constant azimuth (α=0°), diameter ratio (d=10) and offset ratio (b=3). The plane cross-bedded data is always a perfect sinusoid (Fig. 3a). When the dip of the structure increases, the intersection curves for the plane cross-bedded case retain their sinusoidal character, increasing in amplitude, but retaining a constant paleocurrent direction (Fig. 3a). By comparison, the intersection curves for the trough cross-bedded case (Fig. 3b) present a more complex picture. The curves have a sinusoidal style, but are not perfectly sinusoidal. Fig. 3c shows the difference between the plane cross-bedded case and the trough cross-bedded case for plane/trough azimuth of 0°. The difference between the shape of the trough cross-bedded curves and their corresponding plane cross-bedded equivalents depends upon the value of the diameter and offset ratios to such an extent that these curves would not be recognized as sharing the same dips as the associated curve for the plane cross-bedded case in Fig. 3a. However, we can recognize that the trough cross-bedded curves also increase in amplitude as the dip increases, providing the other parameters are held constant. At low dips the apparent paleocurrent direction is not 0° due to the effect of the diameter and offset ratios. However, as the dip increases, the apparent paleocurrent direction, indicated by the minimum in each curve, migrates towards the true value. This is because the high dips compensate to some extent for the perturbation in paleocurrent direction caused by the steep edges of the trough that occur either at large offset ratios or for small diameter ratios (Fig. 3c). Migration of the azimuth (dip direction) with increasing dip angles of the bedding planes is sometimes recognized on electric and acoustic image data plots, and could be indicative of trough cross-bedded sequences. In this case the trough axis direction

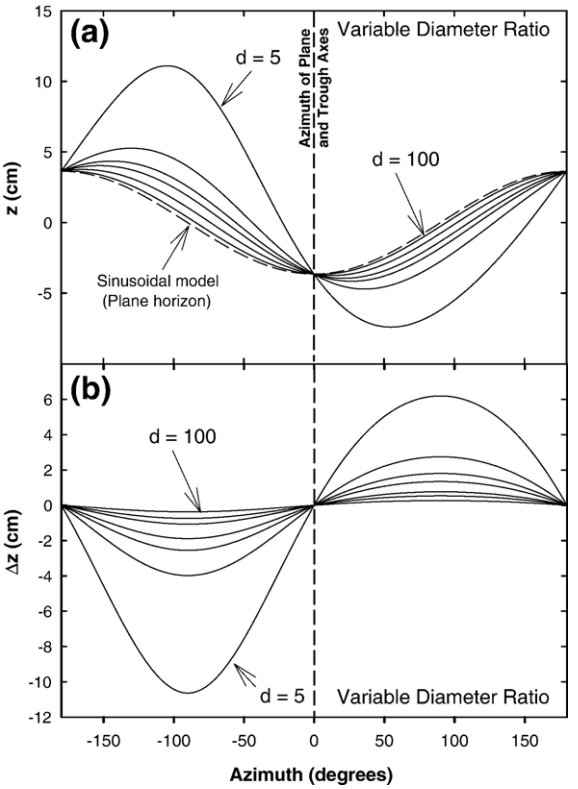

Fig. 4. (a) Forward modeled intersection curves from the trough cross-bedded model (non-planar beds) and the sinusoidal model (planar beds) as a function of diameter ratio (d=5 to 20 in increments of 5, then d=35 and d=100) and azimuth α, with the dip (θ=20°), trough azimuth (ψ_{axis}=0°), and offset ratio (b=3) held constant. The dashed line represents planar behavior. (b) The difference between the sinusoidal model and the trough cross-bedded model as a function of diameter ratio and azimuth α.

(paleocurrent direction) would be closest to the dip azimuth of the bedding plane with the highest dip angle.

Fig. 4a shows intersection curves for the trough cross-bedded case as a function of diameter ratio (d=5 to 20 in increments of 5, then d=35 and d=100), with the dip (θ=20°), azimuth (α=0°), and offset ratio (b=3) held constant. Fig. 4a also shows the intersection curve for the plane cross-bedded case with the same dip and azimuth for comparison. The plane cross-bedded case has $d\rightarrow\infty$ where $z\neq f(b)$ and is shown by the dashed line in the figure. The trough cross-bedded data show significant variations from the plane cross-bedded case at low diameter ratios, but approach the plane cross-bedded case as the diameter ratio increases, as expected. Fig. 4b shows the difference between the plane cross-bedded case and the trough cross-bedded case for plane/trough azimuth of 0°. Once again the effect of a trough-bedded structure is significant. The convergence with the plane case is fairly slow, reaching reasonable correspondence at d=100 (whence the adjusted R^2 statistic calculated by regression reaches 97.85).

Fig. 5a shows intersection curves for the trough cross-bedded case as a function of offset ratio (b=0 to 8 in increments of 1), with the dip (θ=20°), azimuth (α=0 °), and diameter ratio (d=10) held constant. Fig. 5a also shows the intersection curve for the plane cross-bedded case with the same dip and azimuth for comparison. At zero offset ratio, the borehole intersects the axis of the trough. In this case the apparent paleocurrent direction coincides both with its actual value and the value obtained from the plane cross-bedded case. However, the intersection curves will not necessarily have the same shape as those for the plane cross-bedded case depending on the values of the dip and ratio of the radius of the trough to that of the borehole. As the offset ratio increases, the borehole intersects the trough further up the steep sidewall of the

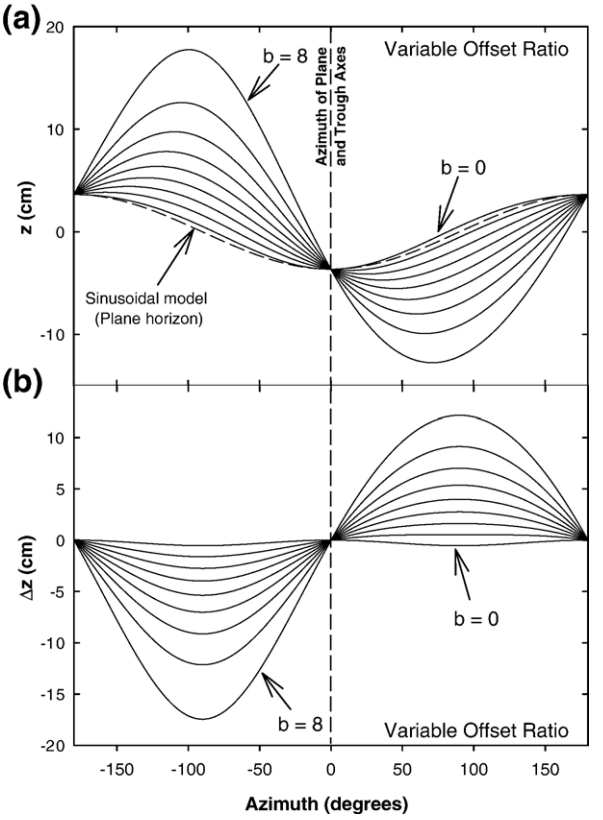

Fig. 5. (a) Forward modeled intersection curves from the trough cross-bedded model (non-planar beds) and the sinusoidal model (planar beds) as a function of offset ratio (b=1 to 8 in increments of 1) and azimuth α, with the dip (θ=20°), trough azimuth (ψ_{axis}=0°), and diameter ratio (d=10) held constant. The dashed line represents planar behavior. (b) The difference between the sinusoidal model and the trough cross-bedded model as a function of offset ratio and azimuth α.

trough, perturbing the apparent paleocurrent direction away from its real value, as can be seen in Fig. 5a, where the minima of successive curves migrate away from 0°. The intersection of the borehole with the steeper trough wall at large offset ratios also leads to an increase in the amplitude of the intersection curves, increasing the apparent dip and leading to large overestimations in dip if a sinusoidal curve is fitted to an intersection curve between a trough cross-bedded structure and a borehole. It should be noted again that the plane cross-bedded case has $d \rightarrow \infty$ where $z \neq f(b)$. This requires that we set $b=0$ in Eq. (1), as shown by the dashed line in the Fig. 5a. Fig. 5b shows the difference between the plane cross-bedded case and the trough cross-bedded case for a structural azimuth of 0°.

Figs. 3–5 show that the trough cross-bedded intersection curves look very similar to the sinusoidal curves expected from planar cross-bedded features. We have fitted sinusoidal curves blindly to a suite of trough cross-bedded intersection curves with known parameters for dips ranging between 5° and 25° and offset ratios ranging from 0.1 to 8.5. The results show extremely good matches with the sum of the root mean squared residuals for the blind sinusoidal fittings within 96% coincidence of the sum of the root mean squared residuals from fitting Eq. (1). The similarity between the two types of curves is smallest for small dips and offset ratios (~96%), increases to reach a peak at about 99.5% at a offset ratio $b=d/2$, and decreases again to ~98.5% as the offset ratio approaches the width of the trough. This implies that the trough cross-bedded curves are often very similar to *some* sinusoidal curve, and blindly fitting a sinusoidal curve to trough cross-bedded data will produce an apparently good fit. The problem is that a sinusoid fitted in this way can be the wrong one in the great majority of cases, and hence provide the wrong dip and azimuth unless the borehole intersects or is close to the axis of the trough by chance.

For example, if we take the trough cross-bedded intersection curves shown in Fig. 5 ($\theta=20°$, $d=10$, $b=4$) and assume wrongly that the structure is planar, the blind fitting of a simple sinusoid gives a difference in the paleocurrent azimuth of +46°, and a difference in dip of +10.6°.

We have calculated the dip by carrying out the best blind sinusoidal fit on a range of trough-bedded intersection curves with actual trough axis dips ranging between 0° and 25°, offset ratios ranging between 0.1 and 6, and for $d=10$ and show the results in Fig. 6. It is clear that large offset ratios can lead to large differences due to blindly fitting sinusoidal curves to trough-bedded data. This must be taken into consideration when using electric or acoustic data to construct dip histograms as such differences could lead to a completely erroneous interpretation of the paleoenvironment when propagated over an entire field.

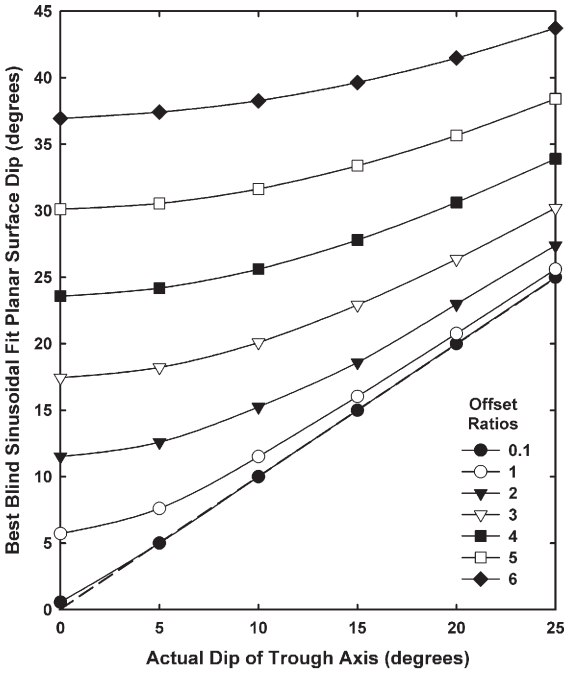

Fig. 6. Apparent trough dip when fitting a simple sinusoidal model to trough data as a function of actual trough dip for various offset ratios and for a diameter ratio $d=10$.

5. How to use the new model

The aim of the analysis is to extract true values of dip θ, trough axis azimuth ψ_{axis}, diameter ratio, d and offset ratio b from each intersection curve. We have developed the following procedure for doing this. First we obtain the largest scale image logs possible. We examine and digitize the images as carefully as possible, remembering that trough cross-bedded curves are similar to plane cross-bedded ones when examined by eye. There are 4 unknown parameters in Eq. (1) (the dip θ, the phase lag φ, the diameter ratio, d and the offset ratio b). It is therefore necessary to have at least 8 digitized points defining each curve. We normalize the curves to the physical scale and then renormalize them to the borehole diameter. Then we can fit Eq. (1) to the data using a non-linear fitting code which provides θ, d, b, and φ. The fitting can be carried out with any commercial curve fitting routine for which the general form of Eq. (1) can be defined. At this stage the trough axis azimuth ψ_{axis} is not derived. If we substitute the derived values of θ, d, b and

φ into Eq. (1) for values of α varying in the range $0 \le \alpha \le 360°$ it is possible to forward-model the intersection curve. The minimum in this curve represents the local direction of maximum gradient α_{min} on the intersected trough surface, which is not equal to the trough axis azimuth ψ_{axis} except when $b=0$ (i.e., the borehole intersects the trough axis), as shown in Fig. 2. However, it is possible to derive the trough axis azimuth ψ_{axis} from the forward modeled curve and its inverse by following the next step (Fig. 7). First we plot the result of equation 1 using the parameters θ, d, b, and φ for values of α varying in the range $0 \le \alpha \le 360°$ (Fig. 7, Curve A). Then we plot the result of equation 1 again on the same diagram, but this time using the parameters θ, *d, minus b*, and φ (Fig. 7; Curve B). These two curves intersect each other twice. One intersection is closer to the minimum of Curve A than the other. Symmetry considerations ensure that the trough axis direction ψ_{axis} is the value of α where the curves intersect that is closest to the minimum in Curve A. In the case of Fig. 7, this is at an azimuth of about 18°. It should be noted that the last procedure assumes only that the trough is axisymmetric.

This procedure provides the values of the parameters θ, d, b, and ψ_{axis} for each intersection curve together with statistical tests for the appropriateness of fit. The values of d and b can then be used together with the borehole radius and the angular data to calculate the actual trough width, borehole offset, and hence the position of each trough or plane structure can be mapped in 3D space.

6. Application to test data

The Formation Micro Imager (FMI) is an electrical image logging tool produced by Schlumberger. We have analyzed a 166 ft (50 m) long section of FMI data with the new technique. The lithologies penetrated consist of fine-grained trough cross-bedded sandstones and shales.

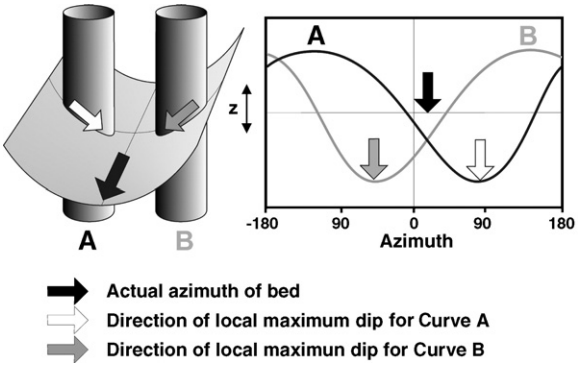

Fig. 7. The derivation of azimuth from fitting by the new model.

The bit-size is 7.875 in. (20 cm). The borehole is on-gauge and of circular cross-section throughout the section. The borehole size controls the FMI borehole surface coverage, and is 55% in this case with the FMI tool in 4 pad mode. The mean structural dip in the section is 14° with an azimuth of 308°, the borehole deviation from the vertical is small (<10°), and the borehole conditions are good.

We examined the data and found 40 possible cross-bedded features. The resistivity images for each feature were digitized, scaled to actual vertical offset and azimuth, and normalized to the borehole diameter. Both the conventional sinusoidal model and the new trough cross-bedded model were fitted to the data using two numerical non-linear fitting engines (NLRG and DATAfit from Oakdale engineering). Two methods were used to ensure that the fitting was reliable.

The parameters derived from each model, together with statistical data indicating goodness and appropriateness of fit are given in Table 1. There is a clear difference in both the dip and azimuth determinations between the two techniques, which is shown clearly by cross-plotting the two techniques (Fig. 8). For dip (Fig. 8a), the sinusoidal method tends to provide larger dip values. This is consistent with the hypothesis that these determinations are affected by local dip caused by the steeper trough sidewalls, and that the use of sinusoidal fitting to trough cross-bedded data introduces inaccuracies in the determination of trough dip. Only five curves give dips that are larger when analyzed by the trough cross-bedded technique, and all of these have very low values of b, indicating that the borehole is intersecting the trough axis.

No apparent correlation exists for the azimuth determinations (Fig. 8b). This behavior also arises from the effect of the steep trough sides that is not accounted for in the sinusoidal model. The expected error in azimuth associated with this effect can be as high as ±90° according to our forward modeling. The gross scatter observed in Fig. 8b indicates that differences in azimuth as large as ±90° are present in practice with only three data points with a difference greater than ±90°, which are erroneous.

The diameter ratios d derived using the new trough cross-bedded model varied from 2.6 (representing a trough 0.52 m wide) to 165 (approaching planar), and the offset ratios b varied from zero (borehole intersecting the trough axis) to 22.7 (borehole 2.27 m from the trough axis). The condition $d > b+1$ (Eq. (A-7)) is honored for all the data which is consistent with all fits being reasonable. Values of low diameter ratio and high offset ratio were associated with a large discrepancy

Table 1
Geometrical and statistical data from analysis of FMI data using the conventional (sinusoidal) and the new (trough cross-bedded) techniques

Curve code	Depth (m)	Sinusoidal method								New method									Type
		θ (°)	ψ_{axis} (°)	Σx^2 (m)×10^{-3}	Standard error (m)	Mean deviation (m)	R^2 (%)	R_a^2 (%)	Durbin Watson coefficient	θ (°)	ψ_{axis} (°)	d	b	Σx^2 (m)×10^{-3}	Standard error (m)	Mean deviation (m)	R^2 (%)	R_a^2 (%)	DurbinWatson coefficient	
1	24.00	7.1	20	12.3	0.022	0.0175	94.36	93.91	0.508	1.1	292	8.6	1.0	4.4	0.014	0.0097	97.96	97.61	0.919	T
2	24.23	21.4	108	27.1	0.030	0.0240	98.83	98.75	0.654	2.5	168	62.2	22.7	26.7	0.031	0.0237	98.84	98.68	0.615	P
3	24.32	18.9	100	13.4	0.020	0.0154	99.33	99.29	0.676	18.9	101	18.8	0.18	10.1	0.018	0.0130	99.50	99.43	0.620	X
4	24.55	6.7	132	18.5	0.023	0.0152	92.97	92.57	0.485	6.1	106	22.3	−1.1	16.9	0.022	0.0156	93.57	92.79	0.544	P
5	24.60	5.1	132	9.26	0.015	0.0150	94.84	94.59	0.436	3.2	174	16.6	1.2	3.7	0.010	0.0075	97.92	97.71	0.868	X
6	27.75	2.3	92	18.6	0.025	0.0188	59.17	56.45	0.471	1.3	10	6.3	0.3	7.0	0.016	0.0124	84.75	82.57	1.126	T
7	27.96	20.2	93	29.2	0.028	0.0249	98.91	98.85	0.407	12.1	146	10.2	2.9	5.0	0.012	0.0083	99.81	99.79	1.368	T
8	28.18	15.0	67	47.3	0.039	0.0284	96.55	96.32	0.460	14.0	87	5.3	0.5	25.1	0.029	0.0219	98.17	97.91	0.640	T
9	28.35	10.3	145	5.4	0.013	0.0095	98.99	98.93	0.846	6.8	73	19.9	3.4	2.4	0.009	0.0067	99.55	99.50	1.545	X
10	28.48	12.2	142	15.4	0.024	0.0182	98.03	97.89	0.421	4.7	75	15.7	3.0	12.2	0.022	0.0173	98.45	98.21	0.562	X
11	28.78	16.1	163	15.4	0.020	0.0160	98.92	98.86	0.658	4.3	88	7.9	2.1	5.2	0.021	0.0085	99.64	99.59	1.665	T
12	28.81	17.4	174	42.3	0.032	0.0244	97.87	97.77	0.445	5.6	102	6.1	−2.0	17.4	0.021	0.0153	99.12	99.03	0.876	T
13	28.90	15.9	153	3.22	0.011	0.0082	99.70	99.68	1.762	14.7	129	165	−17.8	3.2	0.011	0.0082	99.71	99.66	1.775	P
14	35.53	9.3	315	10.8	0.023	0.0171	96.38	96.04	0.754	5.1	11	16.2	−2.1	6.8	0.019	0.0141	97.73	97.25	1.073	X
15	35.57	7.9	2	3.9	0.012	0.0098	98.58	98.47	1.244	5.0	54	20.3	2.2	2.6	0.010	0.0079	99.08	98.92	2.198	P
16	35.73	16.7	1	64.1	0.048	0.0226	95.45	95.12	1.079	11.4	48	8.2	−1.7	55.0	0.046	0.0232	96.09	95.49	1.037	T
17	35.86	14.8	359	39.5	0.039	0.0329	96.52	96.25	0.353	7.4	59	5.8	1.3	11.3	0.022	0.0167	99.01	98.84	0.707	T
18	35.95	9.9	17	36.7	0.037	0.0276	91.28	90.63	0.376	9.3	34	4.7	−0.2	16.1	0.025	0.0159	96.18	95.57	0.908	T
19	41.43	30.4	278	36.3	0.035	0.0275	99.33	99.28	0.385	24.1	319	11.0	−3.6	14.9	0.023	0.0183	99.73	99.68	0.967	T
20	41.47	15.8	327	211.8	0.090	0.0375	83.71	82.46	0.959	12.2	7	16.4	−2.4	210	0.094	0.0357	83.84	81.15	0.932	X
21	41.63	13.8	327	19.4	0.028	0.0218	97.48	97.28	0.683	13.3	342	7.3	−0.4	3.1	0.011	0.0084	99.60	99.53	1.583	T
22	51.68	15.9	153	75.7	0.040	0.0318	99.24	99.20	0.376	30.7	321	13.2	−3.5	68.2	0.039	0.0302	99.31	99.25	0.404	T
23	51.43	33.7	293	18.4	0.023	0.0180	99.36	99.32	0.466	12.5	304	12.5	1.9	10.4	0.017	0.0138	99.64	99.60	0.712	T
24	52.94	23.0	252	10.9	0.017	0.0124	99.55	99.52	0.624	1.9	166	36.5	−11.7	9.1	0.016	0.0118	99.62	99.58	0.676	P
25	53.00	18.8	70	7.0	0.015	0.0118	98.65	98.56	0.707	10.9	89	19.8	−0.2	2.9	0.010	0.0074	99.44	99.36	1.252	X
26	53.55	10.9	93	26.3	0.027	0.0229	99.19	99.14	0.561	19.0	15	13.0	3.0	16.6	0.022	0.0158	99.49	99.42	0.661	T
27	53.82	23.2	51	14.6	0.022	0.0167	99.37	99.33	0.791	13.6	353	17.8	4.1	7.8	0.016	0.0112	99.66	99.62	1.369	X
28	53.92	20.3	46	8.9	0.017	0.0130	99.52	99.48	1.308	2.6	328	30.0	9.1	8.0	0.017	0.0129	99.56	99.50	1.426	P
29	54.02	17.9	15	51.0	0.041	0.0274	97.18	97.00	0.424	14.9	53	31.8	5.8	49.8	0.042	0.0266	97.25	96.85	0.492	P
30	54.11	17.9	19	99.9	0.051	0.0460	96.61	96.43	0.376	19.4	71	5.1	0.7	12.0	0.018	0.0137	99.59	99.55	0.888	T
31	54.16	20.8	50	5.9	0.015	0.0100	99.80	99.79	1.009	16.2	101	20.0	6.3	3.1	0.011	0.0085	99.89	99.88	1.384	X
32	54.27	24.4	71	9.5	0.019	0.0145	99.62	99.59	0.820	18.5	160	27.5	11.3	6.6	0.016	0.0100	99.74	99.69	1.255	P
33	54.37	24.0	44	6.9	0.017	0.0123	99.31	99.25	0.692	9.4	318	18.0	−3.3	3.2	0.012	0.0090	99.68	99.62	1.502	X
34	63.67	15.2	230	263.4	0.088	0.0642	97.98	97.86	0.572	41.6	232	2.6	−.01	95.8	0.055	0.0410	99.26	99.17	1.118	T
35	54.01	42.5	235	2.4	0.008	0.0056	99.70	99.68	0.878	11.7	200	26.3	1.8	1.5	0.007	0.0053	99.81	99.79	1.220	P
36	54.08	12.0	1	46.5	0.034	0.0291	98.05	97.95	0.448	18.5	62	7.5	0.8	8.7	0.015	0.0122	99.63	99.59	0.922	T
37	54.16	19.1	43	18.8	0.022	0.0167	99.54	99.52	0.770	12.6	113	10.1	3.7	1.0	0.017	0.0121	99.76	99.73	1.316	T
38	54.29	25.1	51	28.7	0.031	0.0269	98.40	98.29	0.418	20.5	63	9.2	0.0	8.7	0.018	0.0135	99.52	99.45	1.186	T
39	54.35	20.2	63	18.8	0.024	0.0186	98.95	98.88	0.777	18.6	58	13.1	−0.6	8.2	0.017	0.0131	99.54	99.48	0.974	T
40	54.41	18.8	66	22.1	0.026	0.0191	97.90	97.76	0.445	13.4	13	7.4	0.4	11.7	0.020	0.0145	98.88	98.73	0.724	T

The column labelled θ contains the dip of structure in degrees, that labelled ψ_{axis} contains the azimuth of structure, and d and b are the displacement and offset ratios, respectively. These 4 parameters are derived from the fitting of intersection curves to the digitised data. In the case of the conventional case, only the dip and azimuth are obtained, while the new method provides all four. Statistical tests are shown in the table for the comparison of the best fit model from each method and the digitised data, where Σx^2 is the sum of squares of deviations (i.e. residuals), the standard error and mean deviation are standard measures, and R^2 and $R_a{}^2$ are the ordinary and adjusted regression coefficients, respectively. The Durbin–Watson test is discussed in the text; it tests the applicability of a certain function to a set of data (Montgomery et al., 2001). The codes T, P and X represent our qualitative interpretations of the statistical data, and stand for tough-bedded, plane-bedded and intermediate, respectively.

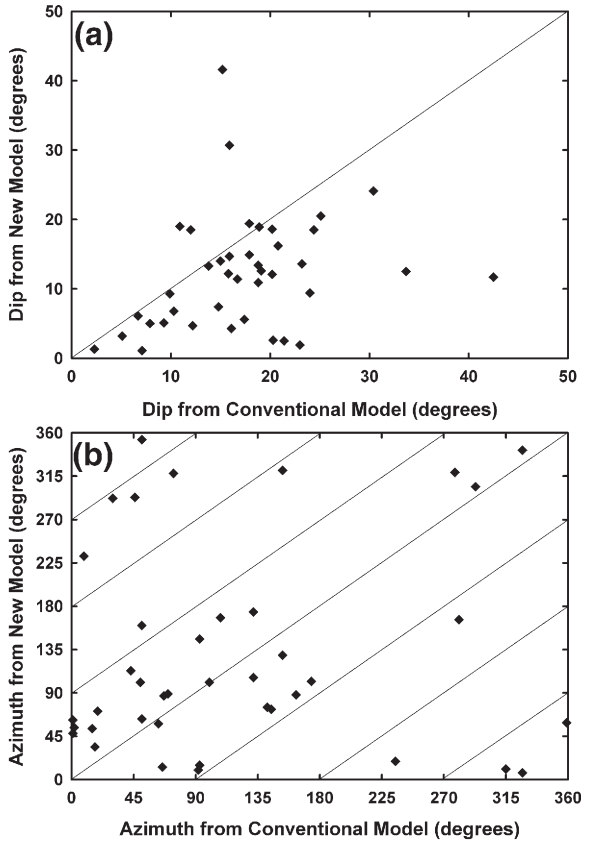

Fig. 8. Crossplots of the (a) dip and (b) azimuth values obtained from the trough cross-bedded model plotted as a function of those obtained from using the sinusoidal method for the test data.

between the dips and azimuths derived from the trough cross-bedded model and the sinusoidal model, indicating that large offset from small troughs was producing large inaccuracies in the dip and azimuth determinations with one or both models. The dip, azimuth, diameter ratio and offset ratios derived from all the curves for both the sinusoidal and new trough cross-bedded models tested are shown in Fig. 9.

We have carried out a number of statistical tests to discriminate whether the trough cross-bedded or the plane cross-bedded model describes each intersection curve best. These statistical tests included: (i) The sum of squares of the residuals from the fit. (ii) The standard error. (iii) The mean absolute deviation (residuals). (iv) The simple coefficient of multiple determination (R^2). (v) The adjusted coefficient of multiple determination (R_a^2), i.e., R^2 adjusted to take account of variations in the number of data points in each fit. (vi) The Durbin–Watson autocorrelation test.

The Durbin–Watson test for autocorrelation (Montgomery et al., 2001) is a statistic that indicates the likelihood that the deviation (residual) values for the regression have a first order autocorrelation component. The regression process assumes that the residuals are uncorrelated. However, if a non-periodic function, such as a straight line, is fitted to periodic data, residuals have a periodic form and are positively correlated over the independent variable (α in this case). These residuals are said to be 'autocorrelated' or 'serially correlated'. The Durbin–Watson tests for autocorrelation in the residuals, and, if discovered, the autocorrelation is an indication that the data is being fitted by an inappropriate function. Small values of the Durbin–Watson statistic (<0.8) indicate autocorrelation, and hence the fitted equation is inappropriate, and large values (>0.8) indicate that the fit is appropriate. If trough data is fitted with a simple sinusoidal curve, the Durbin–Watson statistic tends to zero. This statistic therefore provides a useful tool for discriminating between trough cross-bedded and plane cross-bedded data.

Comparison of the sum of squares of residuals, standard error, mean deviation, R^2 and R_a^2 statistics in Table 1 shows that the new model always fits the data as well as, or better than, a sinusoid. Where the improvement is small, the intersection curve derives from a planar or near-planar structure, and the improvement is due to the increased number of parameters available in the new model (4 parameters; θ, ϕ, b, and d) compared to the sinusoidal model (2 parameters; θ and ϕ). Where the improvement is large, the intersection curve derives from a trough cross-bedded structure, and the improvement is due mainly to the new equation being a much more appropriate one to fit the data. If the improvement in each of these parameters is expressed as a percentage and cross-plotted against the diameter ratio d, strong negative correlations are found, indicating that the improvement in fit is highest for troughs with small diameters, rather than for planar structures.

This scenario is supported by the Durbin–Watson statistics. The arithmetic mean Durbin–Watson statistic of the whole dataset is 0.66 when the sinusoidal model is fitted to the data, but improves to 1.05 for fitting with the new model, indicating that the new model is a much more appropriate function for both the trough cross-bedded and plane cross-bedded data in the dataset.

Examination of Eq. (1) shows that the new model approaches a simple sinusoid at high values of the diameter ratio. It would be expected that the test data would also show that the new model approaches the sinusoidal model as the diameter ratio increases to the point where a trough structure is indistinguishable from a planar structure. If this is the case, one would expect the sum of squares of the residuals of fits with each

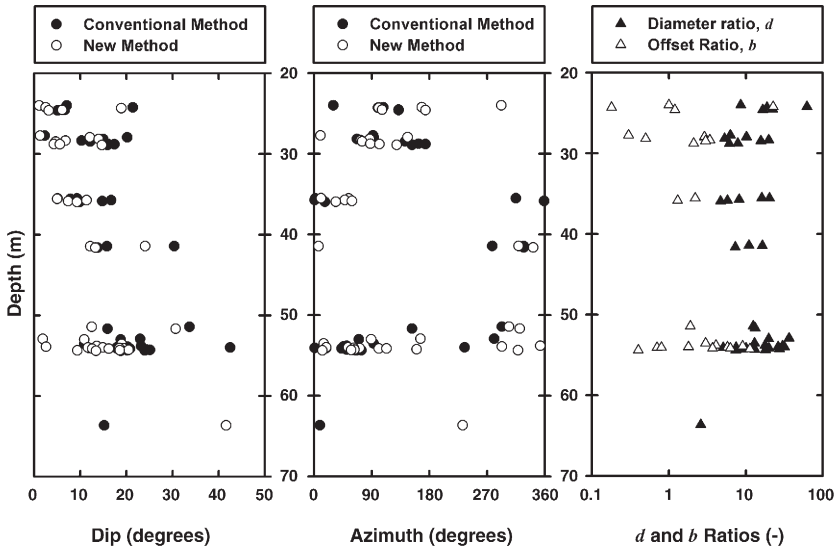

Fig. 9. Dip, azimuth, d, and b ratios as a function of depth for the conventional (sinusoidal) model, and the new (trough cross-bedded) model.

model to each intersection curve to become similar as the diameter ratio increases. We have plotted the difference between (i) the sum of squares of the residuals for intersection curve fits with the new model, and (ii) the sum of squares of the residuals for intersection curve fits with the sinusoidal model, as a function of the diameter ratio (Fig. 10). This figure demonstrates that at small diameter ratios the sum of squares of the residuals from sinusoidal fitting is up to 100 times greater than that from the new model, i.e., the new model is a much better fit to the data. However, as the diameter ratio increases, the difference in the sum of the squares of residuals decreases, until at high diameter ratios there is very little difference in the goodness of fit between the two models, evidenced by their very similar sums of squares of residuals. This indicates that the new model is fitting planar structures well, as well as underlining the necessity to use the new model on trough cross-bedded data.

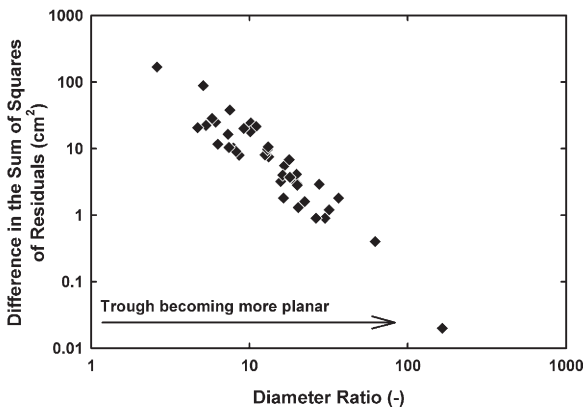

Fig. 10. The difference between the sums of squares of residuals for fits of the conventional (sinusoidal) model to each observed intersection curve and that for fits of the new (trough cross-bedded) model as a function of the diameter ratio obtained from the new model.

The statistics described above, have been combined with the geometrical parameters of dip, azimuth, diameter ratio, and offset ratio, to finally classify the structures represented by each intersection curve as trough cross-bedded or plane cross-bedded (shown in Table 1). In this classification, the primary distinction has been made using the diameter ratio d, where $d>20$ represents planar structures, $d<15$ represents trough cross-bedded structures, and $20>d>15$ represents intermediate structures.

7. Discussion: advantages and limitations

The trough cross-bedding analysis presented in this paper has a number of primary advantages:

First, the dip, azimuth, width and borehole offset of individual trough cross-bedded features can be derived uniquely. This enables the spatial position of individual foresets and set bounding surfaces to be mapped in the sub-surface.

Second, the model can be applied to single features such as turbidite channels, unlike the conventional technique, which relies upon taking the mean directions derived from the analysis of a large number of features to avoid the effect of ambiguity in the borehole offset. Data analyzed using the new technique therefore have a much higher depth resolution than the conventional

technique, being limited only by the occurrence of individual features.

Third, the model can be applied blindly to individual intersection curves from electrical or acoustic image log data containing both plane cross-bedded and trough cross-bedded intersection curves where the dip, azimuth, trough width and borehole offset are not known. This contrasts with the simple sinusoidal fitting technique, which can result in large inaccuracies if fitted blindly to individual intersection curves from electrical or acoustic image log data. If the model is applied to a plane cross-bedded feature the dip and azimuth are reported accurately, and d is reported as a value larger than 20. This value, which we have defined, represents a trough width twenty times that of the borehole (see below).

There are, however, also a number of limitations associated with the technique:

The primary limitation concerns the current resolution of electrical or acoustic image logging tools, which restricts the applicability of the model to troughs with a diameter ratio of less than about 20 (i.e., 3 m for a 20 cm borehole). At diameter ratios greater than this the difference between the trough cross-bedded and plane cross-bedded intersection curves becomes so small that higher resolution image log data are needed for the model to produce accurate values of diameter ratio and offset ratio.

A second limitation is that the borehole diameter must be large enough to resolve the trough cross-bedded feature, but also small enough to maximize borehole surface coverage by the electrical image logging tool in order to maximise the accuracy of the intersection curves. The borehole televiewer (BHTV) does not suffer from this problem.

As always, for best results the borehole conditions need to be good, with a cylindrical borehole cross-section and a lack of caving and break-outs. Any ellipticity in the borehole shape results in intersection curves for plane cross-bedded features that resemble those from trough cross-bedded features. It would be possible to modify the mathematical form of equation 1 to account for ellipticity of the borehole, but this is outside the scope of this paper.

Finally, the depth of investigation for the electrical image logging tools varies depending upon the formation, and can vary azimuthally at a given borehole depth**.** Such a variation could potentially cause intersection curves for plane cross-bedded features that resemble those from trough cross-bedded features.

The model is based on a hemi-cylindrical trough. This is clearly an assumption that may not be true in practice as troughs can be hemi-elliptical in cross-section or filled obliquely. A simple modification in the form of a z-scaling is possible to convert Eq. (1) for use with troughs of an elliptical cross-section. The model has been constructed for a vertical borehole. A simple angular transform would allow Eq. (1) to account for any realistic deviation of the borehole from the vertical.

8. Discussion: implications

It has been the aim of this paper to introduce a new approach to image log data analysis. Maybe a better term would be a modified or extended approach. Certainly the application of a plane model to wells cutting steeply dipping walls of trough-bedded structures has the potential for producing azimuths that are up to ±90° in error in principle. But are these errors commonly occurring in practice? Maybe it is so for single measurements, but conventional analysis uses stacked measurements which reduces the effect of a single outlying value, while also reducing the vertical resolution. The questions that need to be addressed are:

1. Is the real problem as big as the potential problem seems?
2. Does the new method have any real significance in application?
3. Have we been making big interpretive mistakes as a result of using the conventional approach?
4. What are (have been) the consequences of not adopting the method in the real world?

An authoritative answer to these questions can only come from studies of new and existing data where the two methods are assessed and compared blindly. It is best that this were done by the industry as they have easy access to large amounts of data, and are best placed to assess what constitutes a significant discrepancy in results. I would also like to see a comparison carried out on data that had some independent control on the three-dimensional geometry. Such a study may be possible by using the conventional and new methods to analyse image data from a well set a little back from a quarry face that contains trough-bedded features.

9. Conclusions

A mathematical analysis has been carried out on the intersection curves that are possible when a hemi-cylindrical trough with variable diameter, dip and azimuth is intersected by a vertical borehole at some offset from its axis. The analysis has been used to

produce a new model for analyzing image log intersection curves in order to determine paleocurrent directions. The model has been tested on 40 curves from an FMI data suite.

This study has shown that:

- Fitting a simple sinusoidal curve to trough cross-bedded image log data can result in differences in dip as large as +35° and erroneous assessments of azimuth as large as ±90°.
- The new trough model shows deviations from sinusoidal behavior that increase as the dip and the width of the trough decreases, and as the intersection offset between the borehole axis and the trough axis increases.
- The new technique may provide enhanced accuracy in dip and azimuthal determinations for trough cross-bedded structures, although this will need to be independently assessed.
- The new model allows the width of the trough and the offset of the borehole axis from the trough axis to be determined for each intersection curve.
- The new model has an enhanced vertical resolution arising because directional data can be obtained from individual intersection curves.
- The combined information provided by the new model for each curve enables each trough bedded structure to be uniquely mapped in three dimensions in the sub-surface.

The new method has several limitations, primarily that (i) its useful applicability is controlled by the current resolution of electrical or acoustic image logging tools and the size of the borehole, (ii) the borehole should be of good quality with a centralized tool, and there should be no variable depth problems if electrical tool data is used.

Acknowledgments

Grateful thanks are due to Colin McLachlan (Aberdeen University, Mathematics Department), Ian Tribe (Schlumberger Geoquest), J.H. Filancier (Schlumberger Geoquest), Tobi Payenberg (University of Adelaide), Stuart Buck (Z and S Geoscience), S. Luthi (Services Techniques Schlumberger), Andy Siddans (Robertson Geologging Ltd.) and one anonymous reviewer.

Appendix A. The analytical model

In the following mathematical treatment, the parameters that have been used are shown in Fig. 2. It is assumed that the trough can be modeled to a first approximation as an inclined hemi-cylinder, that the borehole can be represented by a vertical cylinder, and that the tool is centralized in the borehole. The assumption of a hemi-cylindrical trough is only required in the close vicinity of the borehole. We use a right-handed cartesian co-ordinate system, the z co-ordinate is vertical, and the xy plane is horizontal. The trough is initially represented by an infinite cylinder of radius d rotated in the xz plane to make an angle θ with the horizontal (xy) plane ($0 \le \theta \le \pi/2$). This object has the equation

$$y^2 + (x\sin\theta + z\cos\theta)^2 = d^2, \; d>1. \qquad (A-1)$$

As only the lower surface of this object is required to represent the trough (i.e., $x\sin\theta + z\sin\theta < 0$) Eq. (A-1) becomes

$$x\sin\theta + z\cos\theta = -\sqrt{d^2 - y^2}. \qquad (A-2)$$

The trough is intersected by a cylinder, representing the borehole, which is coaxial with the z axis. This cylinder is defined to have a radius of unity, implying that the parameter d now represents the ratio of the trough radius to the borehole radius. The intersection can be parameterized as

$$\{(x,y,z) | x = \cos\alpha, y = \sin\alpha\}, \qquad (A-3)$$

where α is the angle with the positive x axis in the xy plane ($0 \le \phi \le 2\pi$) around the borehole diameter with an arbitrary phase lag. The intersection curve can then be written by incorporating the Eq. (A-3) into Eq. (A-2) to give

$$\sin\theta\cos\alpha + z\cos\theta = -\sqrt{d^2 - \sin^2\alpha}. \qquad (A-4)$$

Eq. (A-4) is then solved for z, noting that z now represents the height of the function normalized to the borehole radius (z=actual height of the intersection curve/borehole radius), because of our previous normalization of the diameter ratio, d.

$$z = -\frac{1}{\cos\theta}\left[\sin\theta\cos\alpha + \sqrt{(d^2-1) + \cos^2\alpha}\right]. \qquad (A-5)$$

Eq. (A-5) describes the situation where the borehole axis always intersects the trough axis. This is not commonly true for real applications, and therefore an offset distance, i.e., the perpendicular distance between the trough axis and the intersecting borehole axis must be considered. We incorporate the offset distance as the offset ratio b, which is the offset distance divided by the

borehole radius. Since we only examine the cases where the trough is always completely intersected by the borehole, we can write the condition $d>b+1$.

Introducing the offset ratio b into Eq. (A-5) enables the general equation for the intersection of a hemi-cylindrical trough with a vertical cylindrical borehole to be written as

$$z = -\frac{1}{\cos\theta}\left[\sin\theta\cos\alpha + \sqrt{d^2-(\sin\alpha-b)^2}\right], \qquad (A-6)$$

where z is the height of the function normalized to the borehole radius (z=actual height of the intersection curve/borehole radius), θ is the trough axis dip to the horizontal (xy) plane, α is the angle to the positive x axis in the xy plane, d is the diameter ratio (d=trough radius/borehole radius), and b is the offset ratio (b=offset distance/borehole radius).

Eq. (A-6) has been derived with the trough fixed in the xz plane dipping towards 180°. However, when Eq. (A-6) is used with real image log data we have no *a priori* knowledge of the azimuthal direction of the trough axis. Hence, we must include a phase lag term φ to make Eq. (A-6) useful in practical application. The completely generalized model can then be written as

$$z = -\frac{1}{\cos\theta}\left[\sin\theta\cos(\alpha-\varphi) + \sqrt{d^2-(\sin(\alpha-\varphi)-b)^2}\right]. \qquad (A-7)$$

Examination of Eqs. (A-6) and (A-7) shows that there is only one distinct intersection curve for each set of values of the trough parameters (θ, d, b). Note that the borehole radius does not occur explicitly in this equation because z, d and b are normalized to the borehole radius. Eq. (A-7) could be further generalized to assume a hemi-cylinder with an elliptical cross-section, or to be used with a deviated borehole with little modification.

References

Cameron, I.F., Collinson, J.D., Rider, M.H., Xu, L., 1993. Analogue dipmeter logs trough a prograding deltaic sand body. In: Ashton, M. (Ed.), Advances in Reservoir Geology. Geological Society of London Special Publication, vol. 69, pp. 195–217.

Curray, J.R., 1956. The analysis of two dimensional orientation data. Journal of Geology 64, 117–131.

DeCelles, P.G., Langford, R.P., Schwartz, R.K., 1983. Two new methods of palaeocurrent determination from trough cross-stratification. Journal of Sedimentary Petrology 53, 629–642.

Glennie, K.W., 1972. Permian Rotliegendes of north-west Europe interpreted in light of modern desert sedimentation studies. American Association of Petroleum Geologists Bulletin 67, 1048–1071.

Hurley, N.F., Thorn, D.R., Carlson, J.L., Eichelberger, S.L.W., 1994. Using borehole images for target zone evaluation in horizontal wells. AAPG Bulletin 78, 238–246.

Lofts, J.C., Bedford, J., Boulton, H., Van Doorn, J.A., Jeffreys, P., 1997. Feature recognition and the interpretation of images acquired from horizontal wellbores. In: Lovell, M.A., Harvey, P.K. (Eds.), Developments in Petrophysics. Geological Society of London Special Publication, vol. 122, pp. 345–365.

Montgomery, D.C., Peck, E.A., Vining, G.G., 2001. Introduction to Linear Regression Analysis. John Wiley and Sons, New York.

Pettijohn, F.J., Potter, P.E., Siever, R., 1987. Sand and Sandstone. Springer Verlag.

Rider, M.H., 1996. The Geological Interpretation of Wireline Logs. Whittles Publishing.

Rubin, D.M., 1987. Cross-bedding, bedforms and palaeocurrents. Concepts in Sedimentology and Palaeontology Special Publication, vol. 1. Society of Economic Palaeontologists and Mineralogists.

Robinson, J.W., McCabe, P.J., 1997. Sandstone-body and shale-body dimensions in a braided fluvial system: salt Wash sandstone. AAPG Bulletin 81, 1267–1291.

Scheidegger, A.E., 1965. On the statistics of the orientation of bedding planes, grain axes, and similar sedimentological data. United States Geological Society Professional Paper 525C, C164–C167.

Singerland, R.L., Williams, E.G., 1979. Palaeocurrent analysis in the light of trough cross-bedding stratification geometry. Journal of Geology 87, 724–732.

Trexler, J.H., Cashman, P.H., 1990. Computer assisted palaeocurrent determination from trough cross-stratification. Computers and Geosciences 16, 253–261.